Modeling the Effect of Tissue Displacement during Avascular Tumor Growth on Tumor Progression

Ioannis G. Karafyllidis[1], Dimitra Sasaroli[2], Athanasios Karapetsas[3] and Raphael Sandaltzopoulos[4]

[1] Department of Electrical and Computer Engineering, Democritus University of Thrace,
67100 Kimmeria, Xanthi, Greece

[2] Department of Molecular Biology and Genetics, Democritus University of Thrace,
68100 Alexandroupolis, Greece

[3]Department of Molecular Biology and Genetics, Democritus University of Thrace,
68100 Alexandroupolis, Greece

[4] Department of Molecular Biology and Genetics, Democritus University of Thrace,
68100 Alexandroupolis, Greece,
Email: rmsandal {at] mbg.duth.gr
Corresponding author: Tel.: +30 25510 30622

ABSTRACT – ***We have developed a model for tissue displacement caused by early tumor growth (i.e. before the onset of angiogenesis) using cellular automata and solving diffusion equations on the cellular automaton lattice in order to compute the distribution of oxygen and glucose into the tumor. Tumor growth causes mechanical forces that displace the already existing vessels away from it, thus affecting the distribution of oxygen and glucose which in turn influence tumor growth. We simulated this growth process and we found that tissue displacement may affect tumor progression rate. We also found that the relative distance of the tumor initiation area from neighboring vessels influences its growth. The model and the simulation software we developed can be used to understand the dynamics of early tumor growth and to explore various hypotheses of tumor growth relevant to drug delivery in chemotherapy. Importantly, our approach highlights that vessel displacement should not be neglected in tumor growth models.***

Keywords – cellular automata, tissue displacement, tumor growth, oxygen diffusion, glucose diffusion, avascular growth

1. INTRODUCTION

Data and observations of tumor growth, evolution and adaptability offer strong indications that tumors do not behave randomly, but are self-organized versatile systems able to collect information from their surroundings, alter and exploit their microenvironment and evolve in an organized manner [3, 9, 19]. Tumor growth is a complex phenomenon that integrates genetic, biochemical, chemical and mechanical processes. Tumor growth and tumor induced angiogenesis have been extensively studied and modeled [2, 5, 8, 20, 22]. Here we focus on the modeling of avascular tumor growth, i.e. tumor growth before the neo-angiogenesis phase.

Models for tumor growth can be continuous, discrete or hybrid. Continuous models are based on the use of partial differential equations or stochastic methods and treat the tumor as a (homogeneous or inhomogeneous) continuum surrounded by advancing boundaries. These models actually calculate the velocity and direction of the various tumor boundary points under conditions imposed by the flow of oxygen, nutrients and drugs [5, 6, 8, 10, 22]. In discrete models, the area occupied by the tumor and its environment is divided into small equal areas, thus forming a discrete lattice, and the growth process follows local rules [14, 15, 17, 18]. In this case, tumor growth emerges as a result of the collective behavior of the processes that take place in each of these areas. Discrete models of tumor growth can easily be decomposed in biochemical pathways and provide a useful bridge between the macroscopic tumor behavior and the molecular processes that drive it [12]. Hybrid models combine the discrete models with the solution of partial differential equations on the discrete lattice of these models.

A shortcoming of the tumor growth models is that they do not consider the displacement of the surrounding tissue caused by tumor growth as a basic model parameter. Even prior to the neo-angiogenesis phase, tumor growth exerts

mechanical forces that push any vessels in its vicinity away from the tumor volume, thus inhibiting oxygen and nutrients to reach all tumor cells [13]. This effect enhances hypoxia and possible necrosis in tumor areas. Hence, there is a cycle of events: Tumor growth and the concomitant tissue displacement cause displacement of nearby blood vessels; displacement of vessels alters the distribution of O_2 and nutrients, which in turn affects tumor growth, which affects vessel distances from the tumor and so on. Later on, tumor induced angiogenesis enters this cycle by the production of vascular growth factors such as vascular endothelial growth factor (VEGF) from tumor cells [21] rendering the tumor growth process more complex. It is therefore essential to develop an accurate model of early tumor growth which can serve as a basis and can be extended to incorporate new processes such as angiogenesis and the dynamics of metastasis.

We developed a high level, i.e. tumor level, model and a simulation algorithm based on it, for the study of the effect of tumor growth and tumor induced vessel displacement. We used this algorithm to simulate the growth of a number of tumors that initiated at various distances from a vessel, for the same number of time steps. Simulation results showed that the properties of the physical diffusion processes in the case of moving vessel-tumor boundaries, affect directly tumor progression in the avascular progression phase.

2. MODEL OF TUMOR GROWTH AND TUMOR-INDUCED VESSEL DISPLACEMENT

Normal cells proliferate much slower than tumor cells and the volume of the normal tissue is maintained almost constant because of the balance between cell proliferation and cell death. In our tumor growth model we assume that normal cell proliferation around the tumor has no significant effect on tumor growth. The tumor and the tissue around the tumor are modeled as a two-dimensional cellular automaton lattice. We set each lattice site to correspond to a square with side length equal to *10 μm*, similar to the size of a typical cell. Obviously, if required, lattice dimensions may be adjusted according to our preferences without affecting the mechanics of the algorithm. The state, *S*, of each lattice site rectangle, say the *(i,j)* site, at a time *t*, is the probability that the cell covered by this lattice site rectangle is a tumor cell. The state of a lattice site covering a normal cell is *0* and the state of a lattice site covering a tumor cell is *1*. Lattice sites located at the border between normal and tumor cells have states between *0* and *1*.

During tumor growth the state of a lattice site that is adjacent to the tumor is initially at state *0* and as the tumor grows the state also grows until the state *1* is reached. Tumor growth is modeled as the growth of the states of lattice sites. The state of a lattice site grows at discrete time steps. The state at time step *t+1*, $S_{i,j}^{t+1}$, depends on the states of all neighboring sites at time step *t*, and is calculated according to:

$$\begin{aligned} S_{i,j}^{t+1} &= \left(a\cdot no_{i,j}^{t}+b\cdot ng_{i,j}^{t}\right)S_{i,j}^{t}+\left(a\cdot no_{i-1,j}^{t}+b\cdot ng_{i-1,j}^{t}\right)S_{i-1,j}^{t}+\left(a\cdot no_{i+1,j}^{t}+b\cdot ng_{i+1,j}^{t}\right)S_{i+1,j}^{t} \\ &\quad+\left(a\cdot no_{i,j-1}^{t}+b\cdot ng_{i,j-1}^{t}\right)S_{i,j-1}^{t}+\left(a\cdot no_{i,j+1}^{t}+b\cdot ng_{i,j+1}^{t}\right)S_{i,j+1}^{t} \\ &+0.18\left[\left(a\cdot no_{i+1,j+1}^{t}+b\cdot ng_{i+1,j+1}^{t}\right)S_{i+1,j+1}^{t}+\left(a\cdot no_{i-1,j+1}^{t}+b\cdot ng_{i-1,j+1}^{t}\right)S_{i-1,j+1}^{t}\right. \\ &\quad\left.+\left(a\cdot no_{i+1,j-1}^{t}+b\cdot ng_{i+1,j-1}^{t}\right)S_{i+1,j-1}^{t}+\left(a\cdot no_{i-1,j-1}^{t}+b\cdot ng_{i-1,j-1}^{t}\right)S_{i-1,j-1}^{t}\right] \end{aligned} \quad (1)$$

where $no_{i,j}^{t}$ is the normalized oxygen concentration and $ng_{i,j}^{t}$ is the normalized nutrient (for example glucose) concentration at time step *t* at lattice site *(i,j)*. As described later on in this section, these concentrations are computed at each time step by solving the diffusion equations for oxygen and glucose on the cellular automaton lattice, with boundary conditions that are different for each time step because of the displacement of blood vessels caused by tumor growth. The parameters *a* and *b* are user defined calibration parameters which determine the effect of oxygen and glucose concentration on tumor growth. Indeed, there are experimental ways to define these parameters, but this is not the purpose of our work.

During tumor growth, mechanical forces develop and cause mechanical displacement of the surrounding tissue and blood vessels [4]. In areas relatively away from blood vessels, the concentration of oxygen and nutrients drops almost exponentially with distance. Therefore, the effect of even a minor displacement, which drives vessels away from the tumor, may not be trivial. To model vessel displacement due to tumor growth, we assume that the tissue between the tumor and the vessel is homogeneous and isotropic. We further assume that during the initial phase of tumor growth the forces are not strong enough to cause tissue cell damage, i.e. they do not exceed the elastic limit of the cells, hence the Hooke's law can be applied [11]. Figure 1 depicts vessel displacement caused by tumor growth. Solid lines represent the tumor and vessel borders at present and dashed lines the borders at a previous time point. At the tumor's surface, the forces caused by tumor growth are within normal limits. In Figure 1 the force caused by the displacement AB, acts in the direction of the line AD and causes a vessel displacement CD. According to Hooke's law:

$$\vec{F} = k_{eq}\,\vec{x} \quad (2)$$

where F is the force, k_{eq} is the equivalent elastic constant of tumor and surrounding tissue and x is the total displacement. This displacement comprises the line segments AB and CD. Assuming that the tumor and tissue have different elastic constants, k_c and k_t respectively, the equivalent constant is given by:

$$\frac{1}{k_{eq}} = \frac{1}{k_c} + \frac{1}{k_t} \qquad (3)$$

and the displacement ratio by:

$$\frac{AB}{CD} = \frac{k_t}{k_c} \qquad (4)$$

Since different solid tumors and tissues are expected to have diverse elastic constants, these constants are user-defined parameters in the simulation algorithm which will be described later on.

The results of vessel displacement simulation are shown on Figure 2. Initially, as shown in Figure 2(a), the tumor is relatively small and the forces are not large enough to displace the nearby vessel, but as the tumor grows the vessel is displaced (Figure 2(b)).

Equation (1) relates tumor growth rate with the normalized concentrations of oxygen and glucose, no and ng. Oxygen and glucose diffuse from the vessels and are distributed in the surrounding tissue. Normal tissue and tumor cells uptake oxygen and glucose and act as sinks in the diffusion process. In our model, we choose to use normalized concentrations by setting the values of oxygen and glucose concentrations at lattice sites that are adjacent to vessels equal to *1*. These concentrations are two-dimensional functions that are solutions of the diffusion equations:

$$\frac{\partial no(x,y,t)}{\partial t} = D_{OX}\left(\frac{\partial^2 no(x,y,t)}{\partial x^2} + \frac{\partial^2 no(x,y,t)}{\partial y^2} \right) - U_{OX}(x,y)\ no(x,y,t) \qquad (5)$$

and

$$\frac{\partial ng(x,y,t)}{\partial t} = D_{GL}\left(\frac{\partial^2 ng(x,y,t)}{\partial x^2} + \frac{\partial^2 ng(x,y,t)}{\partial y^2} \right) - U_{GL}(x,y)\ ng(x,y,t) \qquad (6)$$

Equation (5) describes the diffusion of oxygen. D_{OX} is the diffusivity (or diffusion coefficient) of oxygen and U_{OX} is the oxygen uptake rate with units (1/s). Equation (6) describes the diffusion of glucose. D_{GL} is the diffusivity of glucose and U_{GL} is the glucose uptake rate with units (1/s).

We discretize equations (5) and (6) on the cellular automaton lattice and calculate the values of oxygen and glucose normalized concentrations at points that are located at the center of the squares that correspond to lattice sites [1]. Both no and ng are functions of *x*, *y* and *t* and their discrete counterparts used in (1) are:

$$no(x,y,t) \to no^{t}_{i,j} \quad \text{and} \quad ng(x,y,t) \to ng^{t}_{i,j} \qquad (7)$$

Figures 3 and 4 show the distribution of oxygen and glucose, respectively, for the vessel-tumor relative positions depicted in Figure 2(b). The boundary conditions were imposed by setting the values of both normalized concentrations equal to *1* in lattice sites that are adjacent to vessels and equal to *0* in lattice sites that are located more than 200 μm away from the vessel. The diffusivity values are taken to be:

$D_{OX} = 10^{-5}\ cm^2/s$ and $D_{GL} = 10^{-7}\ cm^2/s$ [7]. The uptake rate for oxygen is $U_{OX} = 10^{-1}\ s^{-1}$ and the uptake rates of glucose for normal and tumor areas are $U_{GL} = 10^{-4}\ s^{-1}$ and $U_{GL} = 10^{-3}\ s^{-1}$ respectively [21]. In normal tissue lattice sites, where the state $S=0$, the uptake rate is $U_{GL} = 10^{-4}\ s^{-1}$ and in tumor lattice sites where the state $S=1$, the uptake rate is $U_{GL} = 10^{-3}\ s^{-1}$. In lattice sites that contain both normal and tumor cells the uptake rate is a linear function of the site state *S*. As shown in Figure 4, this results in increasing glucose consumption as we move from normal tissue into the tumor area.

3. SIMULATION OF TUMOR GROWTH AND TISSUE DISPLACEMENT

Based on the model described in the previous section we developed an algorithm for the simulation of the effect of tissue displacement and tumor growth on tumor progression. The flowchart of this algorithm is shown in Figure 5. The user can either draw a hypothetical vessel (or vessels) or import a digitized image of a tissue, in which she wishes to study the dynamics of avascular tumor growth. Then, the user selects a small tissue area (as small as a pixel in the case of an imported image) where the tumor is initiated. If there is already a tumor in the imported image, the user determines

the tumor area as the tumor initiation area. Vessel shape and location and tumor initiation area are the inputs to the algorithm. These inputs also determine the initial and boundary conditions for the tumor growth simulation during the first time step.

After input introduction the algorithm takes the first time step *(t=1)*. Diffusion equations (5) and (6) are discretized and solved on the cellular automaton lattice. Thus the distribution of the normalized oxygen and glucose concentrations, *no* and *ng*, and their values in all lattice sites are determined. These values are used to compute tumor growth using equation (1). Tumor growth causes vessel displacement. This displacement is computed and the new vessel location and shape are obtained. The new vessel location and shape and the new size of the tumor determine the new boundary conditions for the two diffusion equations (5) and (6). The next time step is taken and the diffusion equations are solved with the new boundary conditions determined in the previous time step. The tumor growth, and the new vessel displacement and shape are computed. These will be the new boundary conditions that will be imposed in the next time step and so on until the user determined maximum number of time steps, *Tmax*, is reached. *Tmax* is the time when the avascular phase is supposed to end and the neo-angiogenesis phase begin. Tumor growth causes vessel displacement, which changes the distributions of oxygen and glucose, which in turn affect tumor growth, which causes vessel displacement and this process goes on until neo-angiogenesis is triggered.

We used this algorithm to simulate the growth of a number of tumors that are initiated at various distances from a vessel, for the same number of time steps. We did this for three different pairs of values of the user defined parameters *a* and *b* of equation (1). The results are shown in Figure 6. Line (1) corresponds to *a=0.01* and *b=0.05*. The first tumor initiation lattice site is located 10 μm from the vessel. In our series of digital experiments, this tumor reached the maximum area (maximum size), TA_{max}, in the given time steps. If the size reached by another tumor, say tumor *j*, located further from the vessel in the same number of time steps is TA_j, the normalized size of this tumor, NS_j , is:

$$NS_j = \frac{TA_j}{TA_{\max}} \qquad (8)$$

The normalized size of the tumor that reached the maximum size is *1*. Line (2) corresponds to *a=0.005* and *b=0.03*. Line (3) corresponds to *a=0.001* and *b=0.002*. In each case the growth of fifteen tumors was simulated. The first one is located at a distance of 10 μm from the vessel and the rest fourteen are located at 10 μm intervals at distances ranging from 20 μm up to 150 μm from the vessel. In all three cases, tumor normalized sizes are large at distances from 10 to 40 μm from the vessel. The sizes are reduced significantly at distances from 40 to 70 μm from the vessel and are further slightly reduced at distances from 70 to 150 μm from the vessel.

We attribute these digital experimental results to the nature of the diffusion process. Concentrations of oxygen and glucose are relative high near the vessel, then drop almost exponentially and finally reach a nearly constant minimum value. Our simulation results strongly suggest that the properties of the physical diffusion process in the case of moving vessel-tumor boundaries, affect directly tumor progression during the avascular phase. The values of parameters α and β may vary greatly among different tissues. Therefore, it was not necessary to define the exact parameter values in order to support our main conclusion. Our simulation analysis showed that given any set of parameter values, the vessel displacement affected tumor growth. We should like to stress that it is the *displacement*, not the nature of these parameters that is evaluated by our approach. Therefore, we chose to make our model as general as possible and offer the option to define these parameters according to the properties of the tissue under study.

Based on our analysis, we propose that our model may prove useful in the study of tumor dynamics and consequently the simulation algorithm presented herein may find applications in the study of processes influenced by them, such as optimization of drug delivery strategies [16].

Obviously, the progression of tumor development as a function of time may not be observed experimentally because the dissection of a tumor, at any given time step, requires the sacrifice of the specimen. In addition, technically it is quite difficult to monitor vessel displacement on a tissue section; the plane of the section must pass from the longitudinal axis of the deformed vessel as well as from the solid tumor itself. Analysis is further complicated by the fact that vessels are usually not straight and appear branched. However, we have been able to document vessel distortions and deformations induced by tumor growth during the avascular phase (Supplemental Figure 1). Such observations are consistent with our simulation analysis indicating that tumor growth causes vessel displacement during the avascular phase.

4. CONCLUSIONS

We developed a model and a simulation algorithm for the study of the interplay between tumor growth and tumor induced vessel displacement. Our digital experiments strongly indicated that tumor induced vessel displacement may affect tumor progression. Therefore, our model highlights the importance of taking into account a factor that was overlooked in previous models and urges for experimental validation in a biological system. Furthermore, the model and algorithm can be extended to model tumor growth after the angiogenesis onset by incorporating the diffusion of tumor-

derived angiogenetic factors, such as VEGF, towards the blood vessel and the formation of new vessels. The model presented here can be expanded to three dimensions by considering a 3-D cellular automaton lattice, where the lattice sites will be cubes, and by solving the 3-D diffusion equations for oxygen and glucose on this lattice. This will include the 3-D motion of the molecules and may elucidate further the dynamics of tumor growth and vessel displacement.

Our model and algorithm can be used for the study of various tumor growth scenarios with applications such as understanding early tumor growth dynamics and mechanics, drug and nanoparticles delivery in chemotherapy, access of growth factors and other plasma factors to the tumor, etc.

8. REFERENCES

[1] W.F. Ames, Numerical Methods for Partial Differential Equations, Boston: Academic Press, 1992
[2] R.P. Araujo and L.S. Mcelwain, "A history of the study of solid tumour growth: The contribution of mathematical modelling", Bulletin of Mathematical Biology, vol. 66, pp. 1039-1091, 2004
[3] R. Axelrod, D.E. Axelrod and K.J. Pienta, "Evolution of cooperation among tumor cells", Proceedings of the National Academy of Sciences, vol. 103, pp. 13474-13479, 2006
[4] M.I. Balaguera, J.C. Briceño and J.A. Glazier, "An object-oriented modelling framework for the arterial wall", Computer methods in biomechanics and biomedical engineering, vol. 13, pp. 135-142, 2010
[5] H.M. Byrne, "Modeling avascular tumor growth", Cancer Modeling and Simulation, Ch. 4, ed. Preziosi L, NY: Chapman & Hall, 2003
[6] S. Cui and J. Escher, "Asymptotic behaviour of solutions of a multidimensional moving boundary problem in modeling tumor growth", Communications in Partial Differential Equations, vol. 33, pp. 636-655, 2008
[7] H.B. Frieboes, M.E. Edgerton, J.P. Fruehauf, F.R.A.J. Rose, L.K. Worrall, R.A. Gatenby, M. Ferrari and V. Cristini, "Prediction of drug response in breast cancer using interactive experimental/computational modeling", Cancer Research, vol. 69, pp. 4484-4492, 2009
[8] A. Friedman, Cancer models and their mathematic analysis, in Tutorials in mathematical biosciences, pp. 223-246, ed. Friedman A. , Berlin: Springer-Verlag, 2006
[9] D. Hanahan and R.A. Weinberg, "The hallmarks of cancer", Cell, vol. 100, pp. 57-70, 2000
[10] G. Koch, A. Waltz, G. Lahu and J. Schropp, "Modeling of tumor growth effects of combination therapy", Journal of Pharmacokinetics and Pharmacodynamics, vol. 36, pp. 179-197, 2009
[11] L.D. Landau and E.M. Lifshitz, Mechanics, Oxford: Pergamon Press,1976
[12] J.S. Lowengrub, H.B. Frieboes, , F. Jin, Y.L. Chuang, X. Li, P. MacKlin, S.M. Wise and V. Cristini, "Nonlinear modelling of cancer: Bridging the gap between cells and tumours", Nonlinearity, vol. 23, pp. R1-R91, 2010
[13] P. Macklin and J. Lowengrub, "Nonlinear simulation of the effect of microenvironment on tumor growth", Journal of Theoretical Biology, vol. 245, pp. 677-704, 2007
[14] J. Moreira and A. Deutsch, "Cellular automaton models of tumor development", Advances in Complex Systems Communications in Partial Differential Equations, vol. 33, pp. 247-267, 2002
[15] M.J. Piotrowska and S.D. Angus, "A quantitative cellular automaton model of in vitro multicellular spheroid tumor growth", Journal of Theoretical Biology, vol. 258, pp. 165-178, 2009
[16] B. Ribba, B. You, M. Tod, P. Girard, B. Tranchand, V. Trillet-Lenoir and G. Freyer, "Chemotherapy may be delivered based on an integrated view of tumor dynamics", IET Systems Biology, vol. 3, pp. 180-190, 2009
[17] D. Sabine and A. Deutsch, "Modeling of self-organized avascular tumor growth with a hybrid cellular automaton", In Silico Biology, , vol. 2, pp. 393-406, 2002
[18] A.M. Shnerb, Y. Louzoun, E. Bettlheim and S. Solomon, "The importance of being discrete: Life always wins on the surface", Proceedings of the National Academy of Sciences, vol. 97, pp. 10322-10324, 2000
[19] I. Tannock, R. Hill, R. Bristow and L. Harrington, The Basic Science of Oncology, NY: McGraw-Hill Professional, 2004
[20] P. Tracqui, "Biophysical models of tumour growth", Reports on Progress in Physics, vol. 72, 056701 pp. 1-30, 2009
[21] R.A. Weinberg, The biology of cancer, NY: Garland Science, 2007
[22] D. Wodarz and N.L. Komarova, Computational biology of cancer, London: World Scientific, 2005

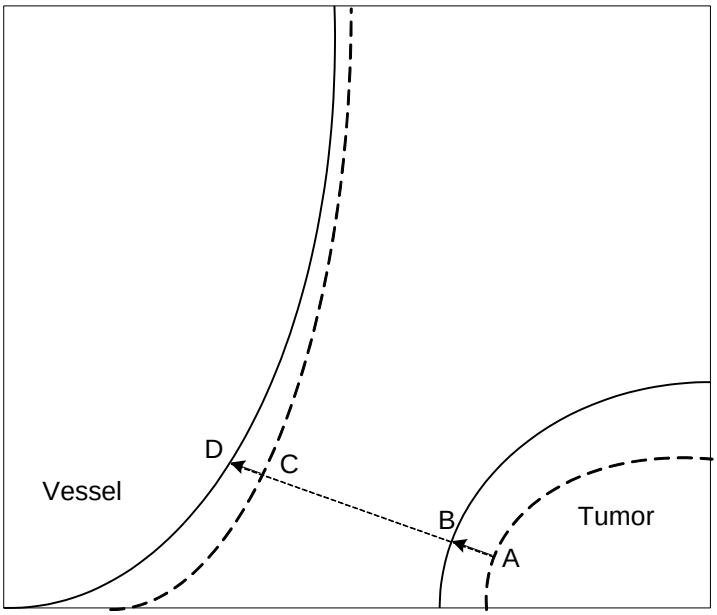

Figure 1. Schematic representation of vessel displacement due to tumor growth. Solid lines represent tumor and vessel borders at present time and dashed lines the borders at a previous time.

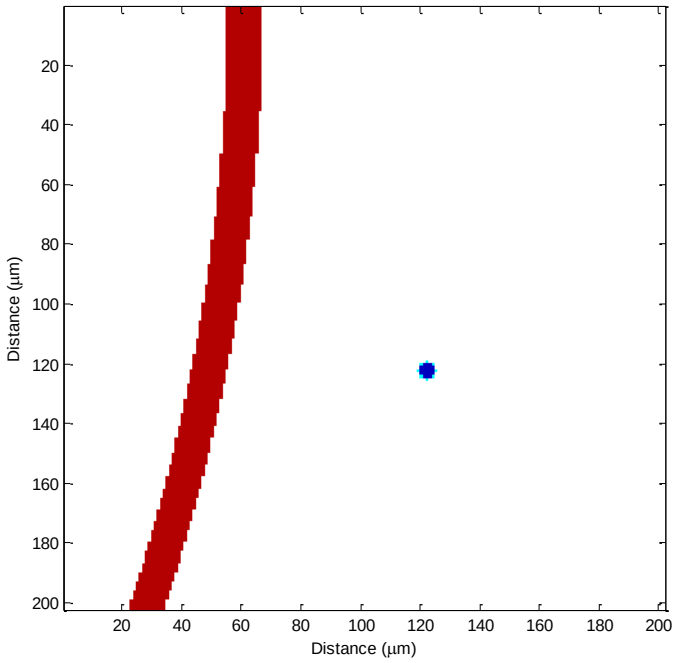

(a)

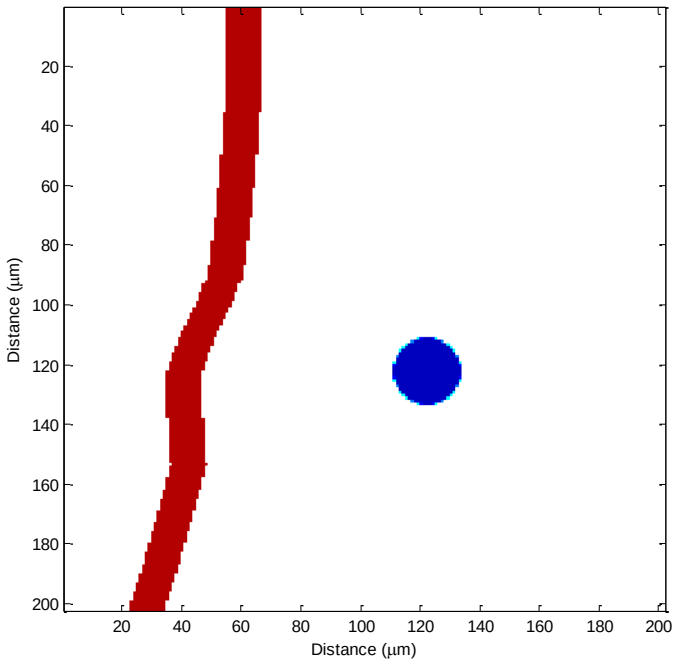

(b)

Figure 2. (Color online) (a) Vessel location and shape at the onset of tumor growth (b) Vessel displaced because of tumor growth.

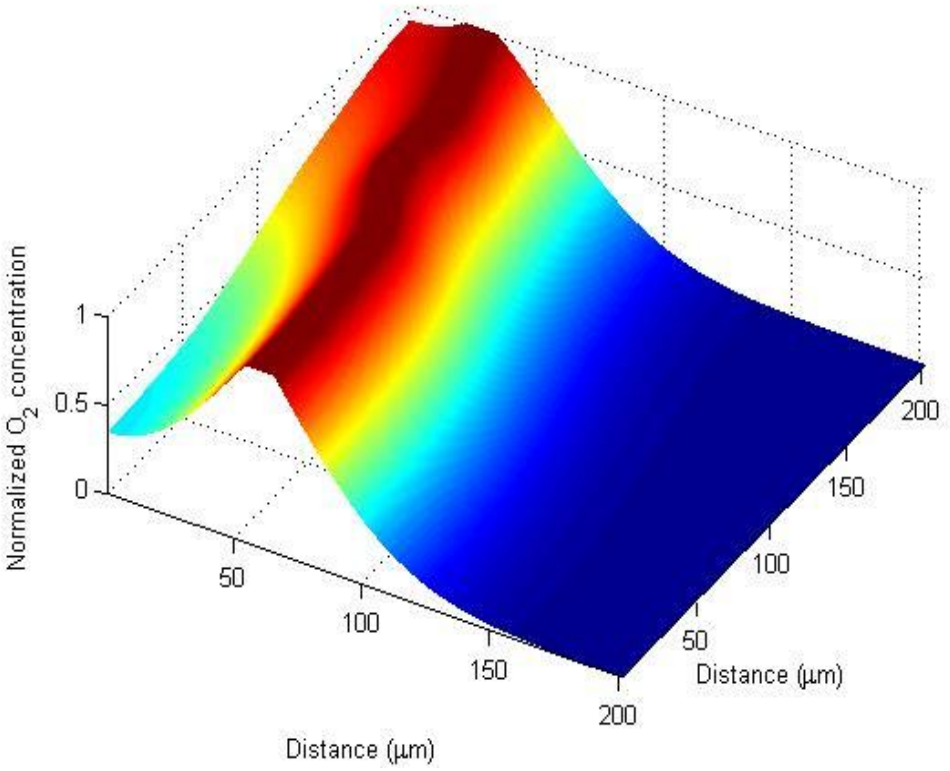

Figure 3. Color online) Distribution of oxygen for the vessel-tumor relative positions depicted in Figure 2(b).

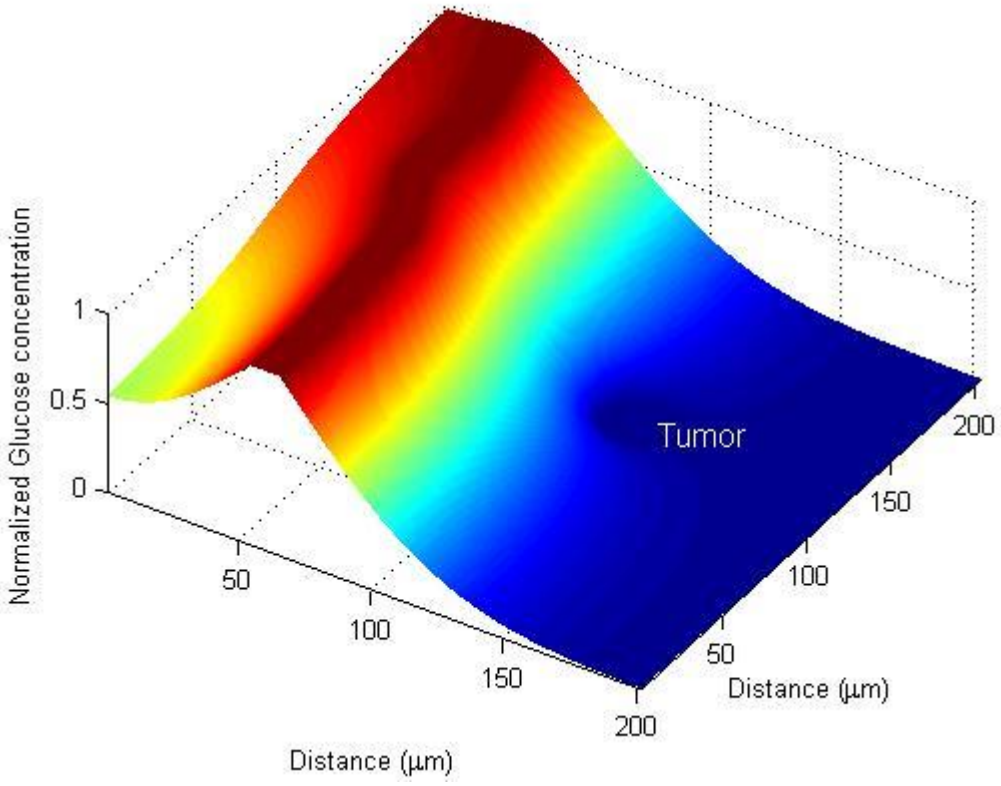

Figure 4. (Color online) Distribution of glucose, for the vessel-tumor relative positions depicted in Figure 2(b).

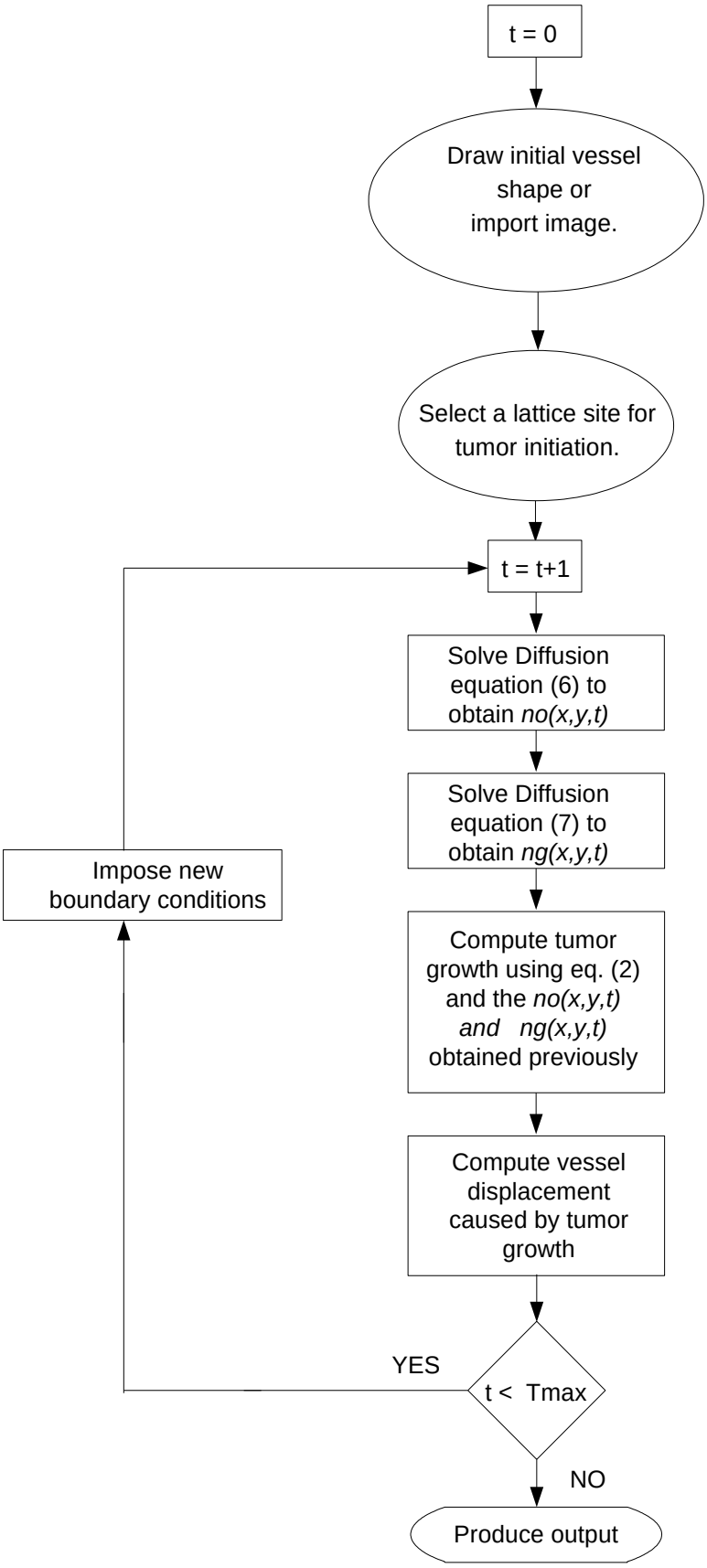

Figure 5. Flowchart of the simulation algorithm.

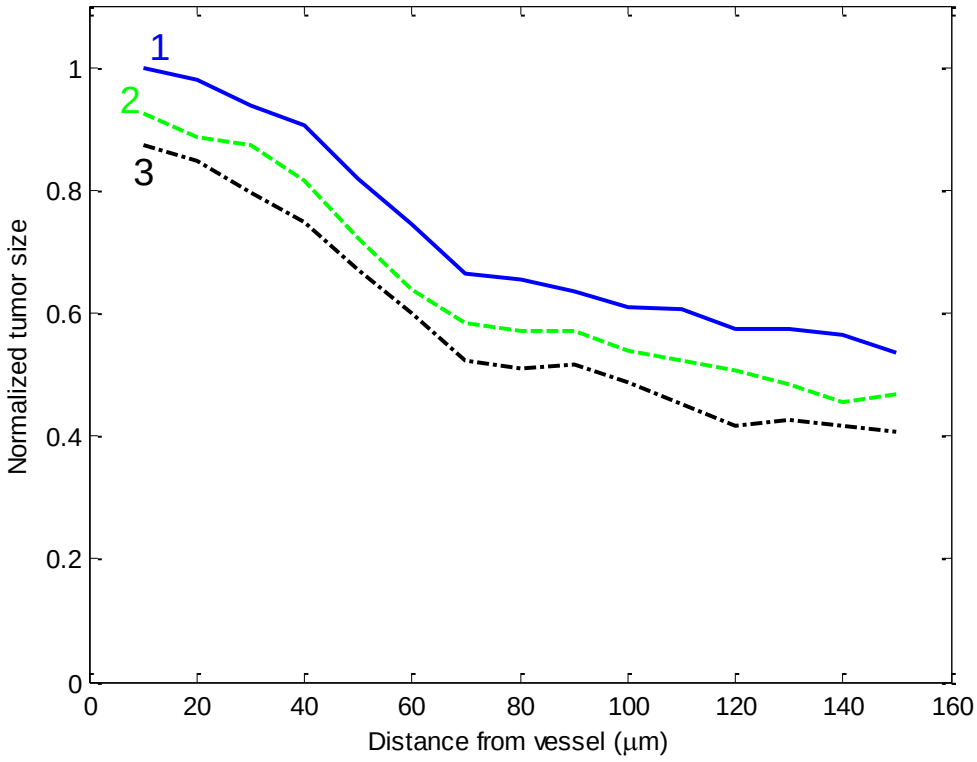

Figure 6. (Color online) Normalized tumor sizes as a function of the distance of the tumor initiation lattice site from the vessel. Line (1) corresponds to a=0.01, b=0.05, line (2) to a=0.005, b=0.03 and line (3) to a=0.001, b=0.002.